Iranian Journal of Oil & Gas Science and Technology, Vol. 4 (2015), No. 1, pp. 35-48
http://ijogst.put.ac.ir

A CFD Simulation of Hydrogen Production in Microreactors

Javad Sabziani and Atallah Sari*

Department of Chemical Engineering, University of Isfahan, Isfahan, Iran

Received: June 07, 2014; *revised:* October 04, 2014; *accepted:* October 15, 2014

Abstract

In this study, the modeling of hydrogen production process in microreactors by methanol-steam reforming reaction is investigated. The catalytic reaction of methanol-steam reforming producing hydrogen is simulated considering a 3D geometry for the microreactor. To calculate diffusion among species, mixture average correlations are compared to Stephan-Maxwell equations. The reactions occurring inside the microreactor include reforming of methanol with steam, methanol decomposition, and a reaction between carbon dioxide and hydrogen. The main objectives of this study are the prediction of temperature profile along the microreactor using either mixture average method or Stephan-Maxwell one and the comparison between the present predictions and some existing experimental data. The simulation results indicate that Stephan-Maxwell method conforms more suitably to the experimental results. The difference is more at lower feed flow rates since, when the flow rate increases, mass transfer mechanism changes from diffusion to convection, which in turn reduces the difference.

Keywords: CFD Simulation, Microreactor, Hydrogen Production, Stephan-Maxwell Equations

1. Introduction

Large quantities of hydrogen are needed in the petroleum and chemical industries, of which the largest application is for the processing ("upgrading") of fossil fuels and in the production of ammonia (Vagia and Lemonidou, 2008, Gallucci and Basile, 2008, Liao and Erickson, 2008). Taking the refining industry into consideration, for example, the hydrogenation occupies over 70% in crude process in America and the ratio is up to 90% in Japan (Fang and Hu, 2006). In addition, hydrogen has increasingly received attention as an energy storage medium which burns in a less-polluting way than do fossil fuels (Ding and Chan, 2006). Firstly, hydrogen has a higher heating value, i.e. 140 MJ/kg, compared to other common fuels (Sharma et al., 2007). Secondly, hydrogen contains no carbon and thus CO_2 is not produced after the combustion. Finally, hydrogen also serves as the ideal fuel for fuel cell, especially for proton exchange membrane (PEM) fuel cell. Therefore, the demand for hydrogen will increase continuously and the cost for hydrogen production becomes crucial.

In recent years, there has been considerable interest in the use of hydrogen as an energy carrier for small fuel cell applications to provide high volumetric and gravimetric energy density for miniaturized portable electronic systems (Fang and Hu, 2006). Hydrogen-fed fuel cells represent high efficiency and negligible pollution. But on-board storing and handling of hydrogen as an on-board fuel is difficult. Also, the storage of hydrogen is not safe. Therefore, the in situ production of

* Corresponding Author:
Email: a.sari@eng.ui.ac.ir

hydrogen on-demand from a liquid fuel in a microreactor is much more desirable. Methanol is an excellent choice as a unique liquid fuel, which is sulfur-free and stored easily. Moreover, the steam reforming of methanol features lower forming temperature and low content of carbon monoxides (Sharma et al., 2007). Since manufacturing of microreactors is costly, their simulation at early stages of manufacturing process is definitely essential toward understanding the physical transport phenomena inside the microreactors and reduces manufacturing costs (Pattekar and Kothare, 2001). Minimization, miniaturization, or micro engineering is a technology which reduces equipment scale, size, and weight while enhances the performance. In this technology, the reduction of characteristic length enhances transport properties, especially heat and mass transfer, which eventually results in enhanced performance. Microchannel structure is similar to monolith reactors. Monolith reactors can be considered as the simplest type of microreactors.

The ability of microreactors to minimize heat and mass transfer resistances led to extensive studies to investigate their industrial feasibility for the production of chemicals. In 2001, Pattekar and Kothare investigated the behavior of a microreactor experimentally and theoretically for in situ hydrogen production from methanol. They simulated the microreactor in 2D with channels of 230 μm×1000 μm. Furthermore, in the study, surface reactions were performed on a thin layer of copper catalyst with a thickness of 33 μm and gas phase reactions were completely ignored. Binary mixture of water-methanol was used to calculate physical properties. The objective of their study was to investigate the effect of operational parameters such as temperature and pressure on methanol conversion, and also to determine the heat required for a continuous process (Pattekar and Kothare, 2001). In 2005, Choi et al. investigated the effect of the number of inlet and outlet flows on methanol steam reforming by the simulation of a microreactor. The simulation was performed in the presence of copper catalyst and assuming plug flow. In the same year, Terazaki et al. experimentally investigated the catalytic methanol steam reforming and compared the required temperature for reaction initiation and the reaction heat loss with the results from the theoretical studies (Terazaki et al., 2005).

In 2005, Kawamura et al. used a 1D model with a spiral flow and considered heat diffusion along the flow direction to find the optimum model for the number of inlet and outlet flows in the production of hydrogen from methanol in microreactors (Kawamura et al., 2005). In 2006, Kim and Kwon investigated a microreactor with six parallel rectangular channels. In their study, all the microchannels are insulated in all the dimensions except one where they are subject to a heat flux. Moreover, the ideal gas behavior was assumed for all the components present in the reaction (Kim and Kwon, 2006).

In 2009, Yakoob et al. experimentally investigated the reaction of methanol steam reforming and compared some catalysts to reduce carbon dioxide production during the reaction. In the same year, Suh et al. used a 1D model to investigate the effect of reaction heating method on the produced carbon dioxide concentration. In this model, heat diffusion was considered along the flow direction (Suh et al., 2009). In 2010, Fazeli and Behnam investigated different geometries to minimize energy consumption using a 2D model for hydrogen production for the catalytic conversion of methanol steam reforming in a microreactor. They assumed a steady state condition and neglected gas phase reactions (Fazeli and Behnam, 2010).

Xuli Zhai et al. (2010) studied the detailed modeling and simulation of a microreactor design for SRM reaction with the integration of a microchannel for Rh-catalyzed endothermic reaction, a microchannel for Pt-catalyzed exothermic reaction, and a wall in between with Rh- or Pt-catalyst coated layer. The elementary reaction kinetics for the SRM process is adopted in the CFD model,

while the combustion channel is described by global reaction kinetics. The model predictions were quantitatively validated by the experimental data in the literature. For the extremely fast reactions in both channels, the simulations indicated the significance of the heat conduction ability of the reactor wall as well as the interplay between the exothermic and endothermic reactions (e.g., the flow rate ratio of fuel gas to reforming gas). The characteristic width of 0.5 mm is considered to be a suitable channel size to balance the trade-off between the heat transfer behavior in microchannels and the easy fabrication of microchannels (Xuli et al., 2010).

Binlin Dou and Yongchen Song (2010) have been simulated hydrogen production from the steam reforming of glycerol in a fluidized bed reactor using a CFD method by an additional transport equation with a kinetic term. The Eulerian-Eulerian two-fluid approach was adopted to simulate the hydrodynamics of fluidization, and the chemical reactions were modeled by a laminar finite-rate model. The bed expansion and pressure drop were predicted for different inlet gas velocities. The results showed that the flow system exhibited a more heterogeneous structure; the core annulus structure of gas-solid flow led to back-mixing and internal circulation behavior, and thus resulted in a poor velocity distribution. This suggests the bed should be agitated to maintain satisfactory fluidizing conditions. Glycerol conversion and H_2 production were decreased with increasing the inlet gas velocity. An increase in the value of steam to carbon molar ratio increases the conversion of glycerol and H_2 selectivity. H_2 concentrations in the bed were uneven and increased downstream; high concentrations of H_2 production were also found on walls. The model demonstrated a relationship between hydrodynamics and hydrogen production, implying that the residence time and steam to carbon molar ratio were important parameters (Binlin and Yongchen, 2010).

Irani et al. (2011) investigated and compared two approaches toward reaction modeling in monolith reactors. In the first approach, the reactions are assumed to take place on the wall surfaces, while penetration and the reaction of chemical species inside a thin layer near the walls are of essential concern in the second approach. The experiments of steam methane reforming (SMR) were carried out in a bench-scale monolith reactor. A single-channel was considered and two axi-symmetric CFD models were developed for modeling. General kinetic models for SMR and water-gas-shift reaction (WGSR) rates based on Langmuir-Hinshelwood type were employed. Comparisons between modeling results and experimental data showed that, despite its ease of implementation, the first approach (surface reactions) exhibited better results both in terms of generality and accuracy. It was realized that uncertainties in obtaining the effective diffusion coefficients in the volumetric approach might cause a variation up to 16% in the prediction of reaction conversion (Irani et al., 2011).

It appears that the existing studies employ mostly rather simple models and mixture average correlations are used to calculate diffusion between species. Relatively little work has been done on the three-dimensional full model analysis. Therefore, in this study, the results of Stephan-Maxwell equations are compared to that of mixture average correlations using a 3D model. The objective of the study is a CFD simulation of the behavior of hydrogen producing microreactors.

2. Mathematical model

2.1. Process description

In this study, the behavior of a microreactor, which produces hydrogen by methanol steam reforming, is modeled and simulated considering the interaction of transfer phenomena, flow hydrodynamics, and conversion reaction kinetics. A microreactor with dimensions of 1 mm×0.5 mm×20 mm including

six microchannels is selected for the simulation of hydrogen production from methanol. Geometric structure of the microreactor is shown in Figure 1.

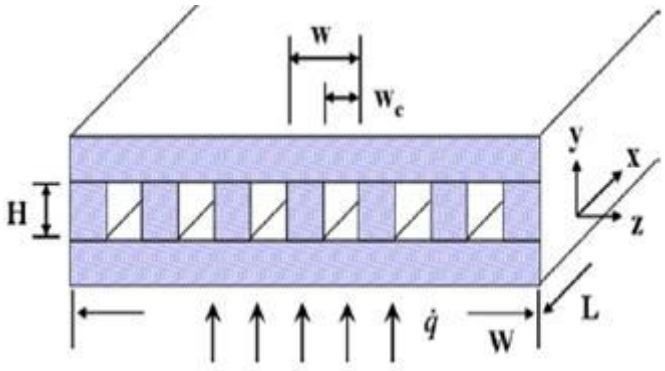

Figure 1
The geometric structure of the microreactor.

$Cu/ZnO/Al_2O_3$ is used as the catalyst, which is coated on the bottom of the channels. All the surfaces are insulated except the one on the bottom, which is subject to a heat flux. The reactant distribution is to be uniform; therefore, the results are the same for all the channels and the results are presented just for one channel.

2.2. Kinetics of the reaction rate equations

The reactions include methanol steam reforming, methanol decomposition, and the reaction between carbon dioxide and hydrogen.

$$CH_3OH + H_2O \rightarrow 3H_2 + CO_2 \tag{1}$$

$$CH_3OH \rightarrow CO + 2H_2 \tag{2}$$

$$CO_2 + H_2 \rightarrow CO + H_2O \tag{3}$$

The rate equations of the above reactions are as follows (Fukahori et al., 2008, Mizsey et al., 2010):

$$r_1 = k_{10} C_{CH_3OH}^{0.6} C_{H_2O}^{0.4} \exp\left(-\frac{E_{a_1}}{RT}\right) \qquad \frac{mol}{(m_{cat}^3.s)} \tag{4}$$

$$r_2 = k_{20} P_{CH_3OH} \exp\left(-\frac{E_{a_2}}{RT}\right) \qquad \frac{mol}{(g_{cat}.s)} \tag{5}$$

$$r_3 = k_{30} C_{CO_2} C_{H_2} \exp\left(-\frac{E_{a_3}}{RT}\right) \qquad \frac{mol}{(m_{cat}^3.s)} \tag{6}$$

2.3. Equations of model

The equations of conservation of mass, momentum, and energy are used. This model has been scaled up to a certain geometry size and has been used to integrate the kinetics of the chemical reactions

involved into the CFD model. Figure 2 shows the element in the center of a microreactor with the cubic geometry.

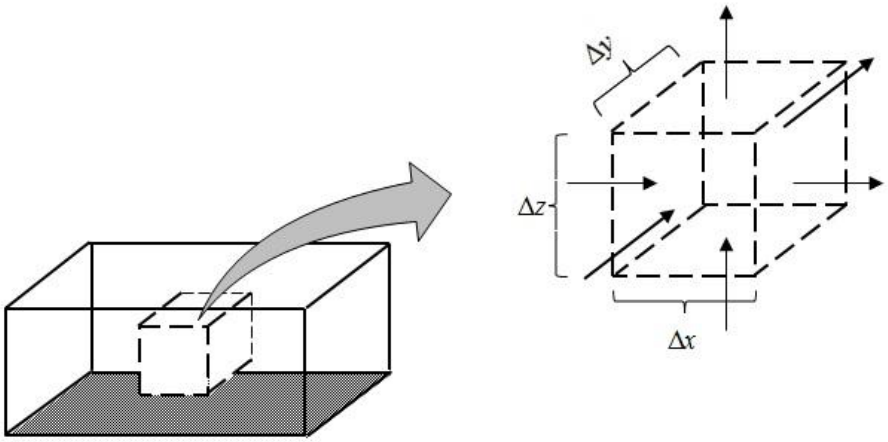

Figure 2
Volume element in center of microreactor.

The following assumptions were made for the simulation:

1. All the components are in gas phase;
2. Fluid flow regime is considered to be laminar;
3. The reactor is considered to operate in steady state condition;
4. The catalyst layer is homogeneous and isotropic, and the reaction occurs just on catalyst surface;
5. The microreactor is insulated in all the dimensions except one dimension, which is subject to a heat flux;
6. The flow of the reactants is assumed to be ideal due to high temperature and low pressure.

The equation of conservation of mass for each component is written considering Stephan-Maxwell equations and mixture average correlations. Total flux for each component is defined according to Equation 7:

$$N_i = J_i + \rho u \omega_i \tag{7}$$

where, N_i, J_i, ρ, u and ω_i are total flux, diffusion flux, density, velocity, and mass fraction respectively. Mass conservation for each component is given by:

$$\nabla . J_i + \rho (u . \nabla) \omega_i = R_i \tag{8}$$

where, R_i is production or consumption due to chemical reaction.

To calculate the diffusion flux of each component, two methods are used. Considering Stephan-Maxwell equations, it can be written as:

$$J_i = -(\rho \omega_i \sum_k D_{ik} d_k + D_i^T \frac{\nabla T}{T}) \tag{9}$$

where, D_{ik} represents the diffusivity of *i* inside *k* and the last term is diffusion due to temperature gradient. d_k is the mass transfer driving force:

$$d_k = \nabla x_k + \frac{1}{P_A}\left[(x_k - \omega_k)\nabla P_A\right] \tag{10}$$

where x_k reads as:

$$x_k = \frac{\omega_k}{M_k} M_n \tag{11}$$

$$M_n = (\sum_j \frac{\omega_j}{M_j})^{-1} \tag{12}$$

It also uses mixture average correlations as follows (i.e. *x* direction):

$$J_{kx} = -D_{km} \frac{\partial \rho_k}{\partial x} \tag{13}$$

D_{km} represents diffusivity of *K* inside the fluid bulk. The general equation of conservation of momentum is defined as:

$$\rho(U.\nabla)U = -\nabla\pi + \rho g + F \tag{14}$$

where, π, g, and F represent momentum molecular flux, gravity, and external force respectively. The first term represents momentum variation due to convection, the second term includes pressure and viscous forces, and the third and fourth terms show the effect of external forces per volume unit.

Moreover, the equation of conservation of energy is given by:

$$\rho c_p u.\nabla T = \nabla.(k\nabla T) - \nabla.(\sum_k h_k J_k) + Q_{reaction} \tag{15}$$

In this equation, *h*, *k* and C_p are enthalpy, thermal conductivity, and heat capacity respectively. The first term represents energy variation due to convection, while the second term shows energy change due to conduction; the third term is enthalpy change as a result of diffusive mass flux; the last term stands for energy source due to reaction. In this equation, the reversible and irreversible changes in enthalpy due to pressure and viscosity are neglected.

2.4. Boundary conditions and model parameters

The boundary conditions at the inlet and outlet of the reactor are considered. Table 1 gives the boundary conditions in the simulations.

It should be noted that in the energy conservation equation, Q_R is the heat of reaction and *q*" represents the heat flux applied to the microchannel wall.

Table 1
Boundary conditions in the simulations.

Equation	Boundary conditions	
Continuity Equation	Input $\rightarrow v_x = v_{0x}, \quad v_y = v_{0y}, \quad v_z = v_{0z}$	
Components Conservation	Input $\rightarrow C = C_0$	Out put $\rightarrow \nabla . J_k = 0$
Components Conservation	Input $\rightarrow \omega_k = \omega_0$	Out put $\rightarrow n.\rho\omega \sum_k B_{ik} d_k = 0$
Momentum Conservation	Input $\rightarrow v_x = v_{0x}, \quad v_y = v_{0y}, \quad v_z = v_{0z}$	Output $\rightarrow v_x = v_{xl}, \quad v_y = v_{yl}, \quad v_z = v_{zl}$
Energy Conservation	Input $\rightarrow T = T_0$	Out put $\rightarrow -n.(-k\nabla T) = q^{"} + Q_R$

2.5. Solution scheme

The governing Equations 7-15 which describe fluid dynamics, heat and mass transfer, and reaction behaviors in the gas phase are solved numerically. COMSOL 4.2 is used to solve the NeS equations describing the flow field behaviors. It is performed with the aid of self-developed C codes and the semi-implicit discrete method is used to solve these stiff equations successfully (Bader and Deuflhard, 1983). The global kinetics of reaction is also solved by self-developed C codes. User-defined functions (UDF's) provided by COMSOL 4.2 are used to provide the solver of stiff equations with the information of temperature and concentration in the flow field, which serves as the initial values. The mass and energy fluxes of species in the gas phase are obtained from the solution of stiff equations and returned to COMSOL 4.2 and used to calculate the flow field by UDF's. For solving the model equations by a software package, the microreactor was divided into a mesh. Maximum mesh size was 0.1 mm and capable of auto adaptive; so, if the region of microreactor gradients is severe, the mesh dimensions are small and vise versa. A view of the microreactor initial mesh in channel is shown in Figure 3.

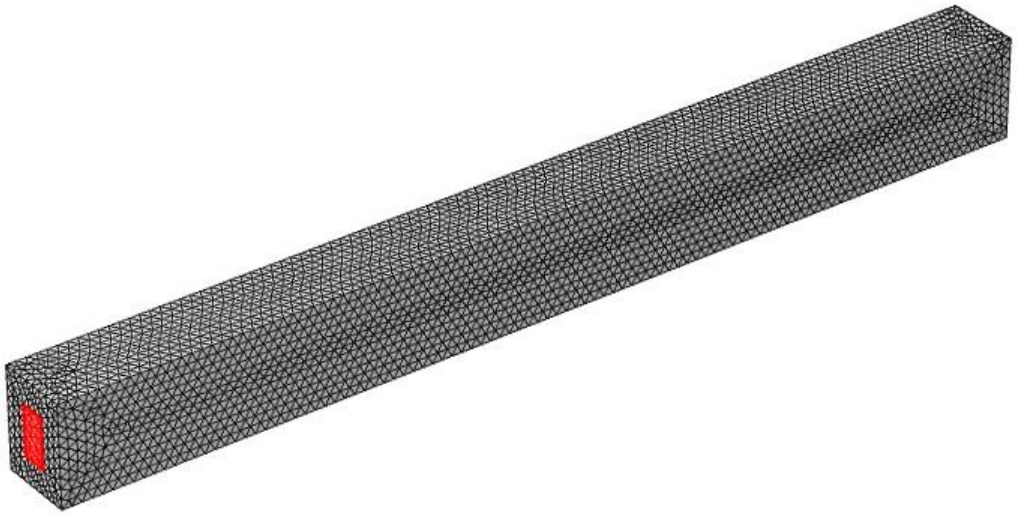

Figure 3
The microreactor initial mesh.

To achieve the optimum mesh size in each run, velocity in the channel center was considered. By reducing the mesh size and thus increasing the mesh elements, the changes in the velocity are monitored and when no change is seen the mesh size is considered as the optimal size. Velocity changes in the channel center according to the number of mesh elements are provided in the following table.

Table 2
Velocity changes in the channel center according to number of mesh elements.

Maximum mesh size (mm)	Number of mesh elements	Outlet velocity(center of channel) (mm/S)
0.2	70123	4075
0.1	82132	4277
0.09	127934	4279
0.07	194123	4312
0.05	228410	4319
0.03	301232	4326
0.01	375239	4331

As it is clear from Table 2, by reducing the maximum mesh size of 0.1 mm, the number of mesh elements and also computational time greatly increases, while a significant change is not seen in the velocity as a result. Thus a mesh size of 0.1 mm is considered as the optimal size of mesh.

3. Results and discussion

For presenting a three-dimensional channel as two-dimensional, in each cross section, the average of the desired result has been taken using the surface integral. In other words, each point on the graph represents a cross-section of a medium.

First, for comparison with the experimental results, the simulation is performed for the inlet flow rates of 1 ml/s, 3 ml/s, and 5 ml/s for water and methanol. The temperature profiles are shown in Figures 4 for mixture average correlations, Stephan-Maxwell equations, and the experimental data.

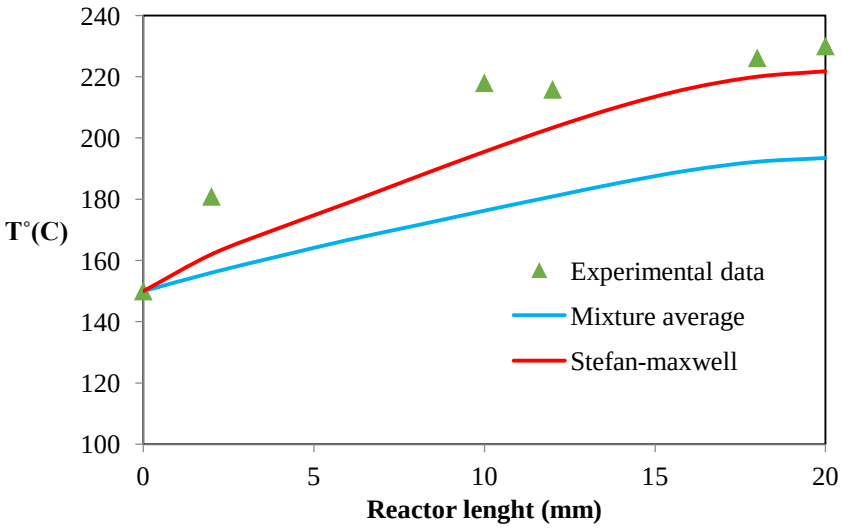

Figure 4
Comparison of temperature profiles along the microreactor for mixture average correlations, Stephan-Maxwell equations, and the results obtained for the experiment at a flow rate of 1 ml/s (Kim and Kwon, 2006).

Figure 4 shows the distribution of the temperature with a change in the ratio of steam to the entrance methanol. At the equal molar ratio of methanol to steam in the feed, because feeds are available for reaction all along the channel, the hydrogen production rate is higher in the output and the temperature in the channel length is less than the other ratio; by changing this ratio as a part of the channel, the reaction conversion is not done. Furthermore, the hydrogen production rate decreases, while temperature increases along the channel.

The relative error in temperature profile prediction at different flow rates are tabulated in Table 2.

Table 3
Relative error in temperature profile calculation at different flow rates.

Flow rate (ml/s)	Mixture average correlations	Stephan-Maxwell equations
1	18.7	6.8
3	10.95	5.7
5	5.9	4.0

As it is obvious, the relative error is higher in mixture average correlations than Stephan-Maxwell equations at all the flow rates, and as the flow rate increases, the relative error of mixture average correlations decreases compared to Stephan-Maxwell equations. This is well illustrated in Figure 5. It is clear that by increasing flow rate, the ratio of H_2 conductive to convective flux is greatly reduced and convection is the mechanism of mass transfer. As a result, the relative error of mixture average correlations is close to Stephan-Maxwell equations.

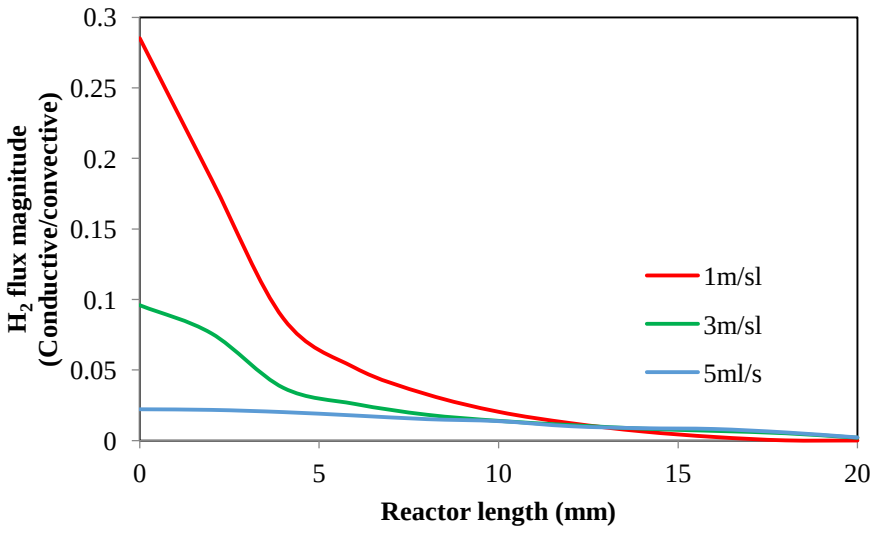

Figure 5
H_2 conductive to convective flux at different flow rates.

Additionally, methanol mole fraction along the channel is shown in Figure 6.

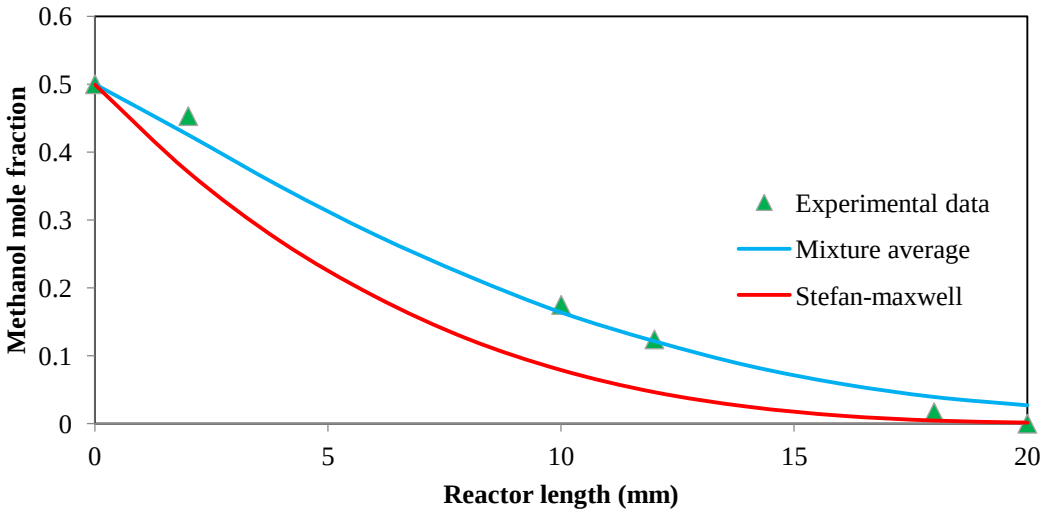

Figure 6
Comparison of methanol mole fraction profiles along the microreactor for mixture average correlations, Stephan-Maxwell equations, and the results obtained for the experiment at a flow rate of 1 ml/s (Kim and Kwon, 2006).

As it is shown in Figure 6, in the prediction of mole fraction profiles of methanol, Stefan-Maxwell theory has a relative error smaller than mixture average relationships. Moreover, at the beginning of the channel, the reaction rate of conversion is higher and thus the mole fraction of methanol is reduced more rapidly; but with advancing along the channel and thereby the reduction in the concentration of the reactants, the reaction rate decreases and finally at the end of the channel the mole fraction of methanol is almost constant.

Figure 7 shows the temperature changes during microreactor in a contour plot.

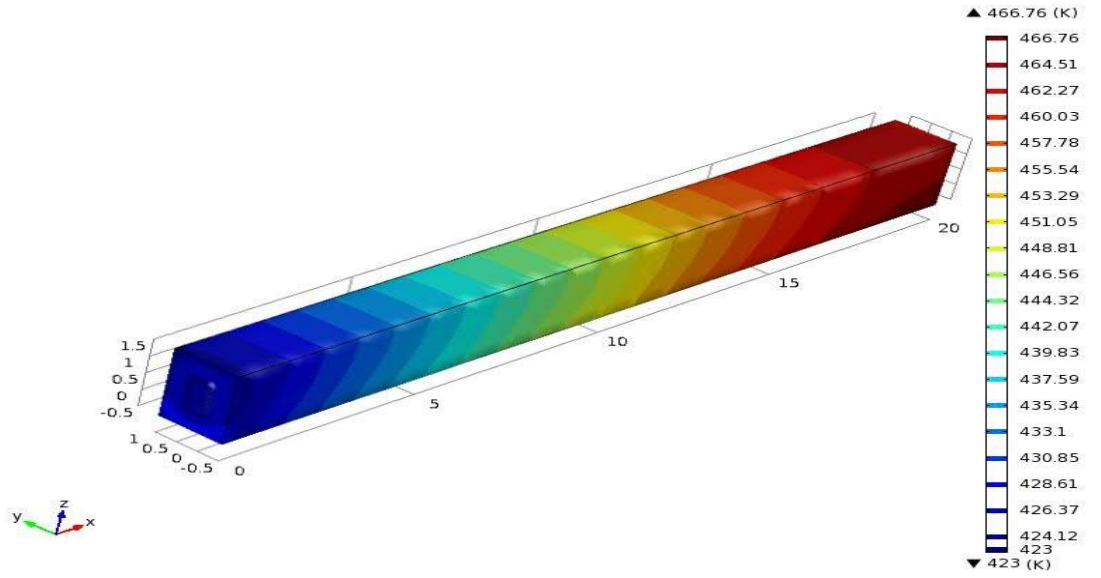

Figure 7
The temperature contour.

As it is inferred from Figure 7, due to the decrease in the reagents during microreactor and the applied constant flux, the temperature rises continuously over the channel and reaches its maximum value at the output. In addition, Figures 8 and 9 show velocity and methanol concentration contours respectively.

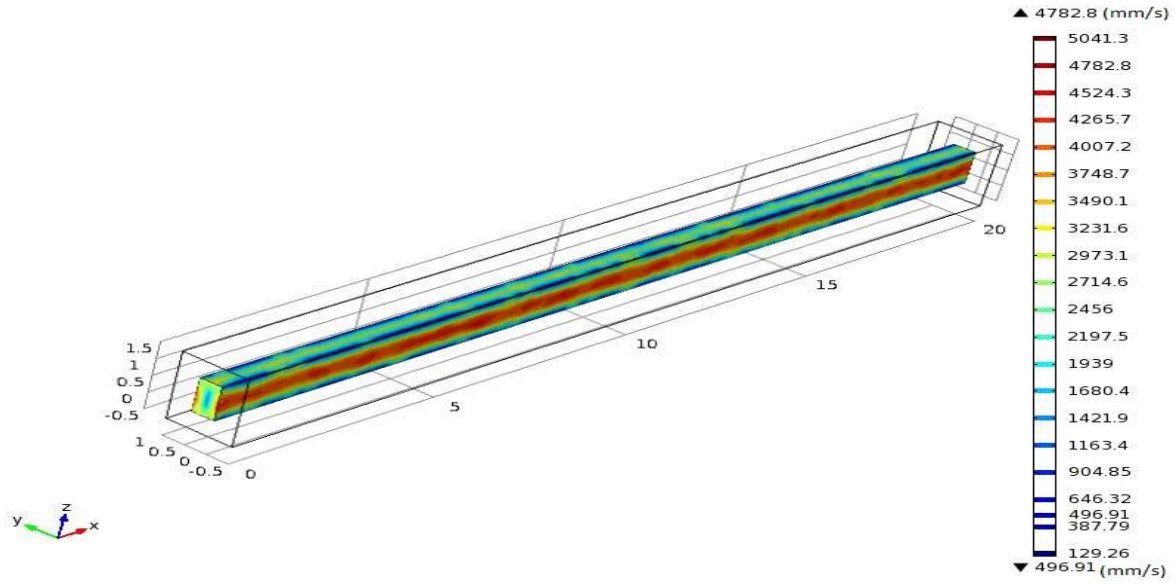

Figure 8
The velocity contour.

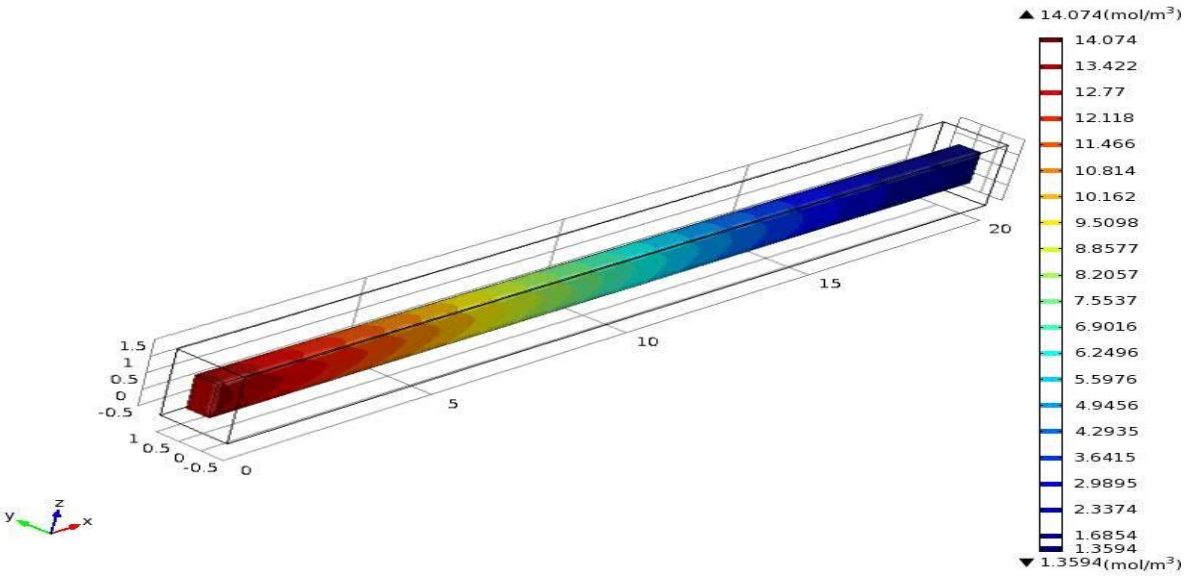

Figure 9
The methanol concentration contour.

As it is seen in Figures 8 and 9, the maximum velocity happens in the center of the channel while it reaches zero on the wall; methanol concentration also decreases throughout the channel.

To evaluate the efficiency of the reaction, the mole fraction of methanol and hydrogen production yield were used as the two main criteria. Hydrogen production yield and hydrogen selectivity are respectively defined by:

$$Y_{H_2} = \frac{n_{H_2,out}}{n_{CH_3OH,in}} \tag{16}$$

$$S_{H_2} = \frac{n_{H_2,out}}{n_{H_2,out} + n_{H_2O,out}} \tag{17}$$

The variation of hydrogen production yield along the channel is displayed in Figure 10.

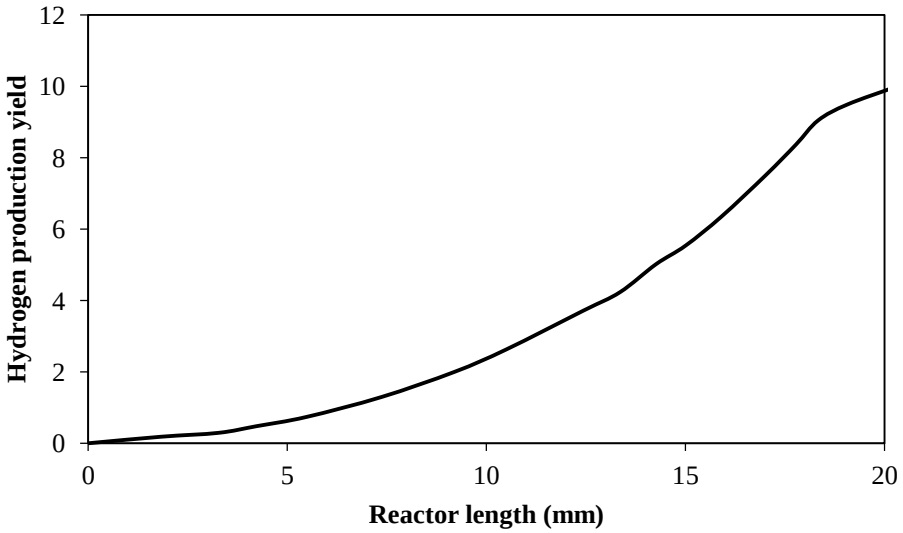

Figure 10
Hydrogen production yield along the channel.

Hydrogen production yield illustrates the number of moles of hydrogen produced per mole of methanol; since the number of moles of hydrogen produced rises during the channel, the maximum rate of hydrogen production is at the output, where it reaches 11%.

4. Conclusions

In this study, mixture average correlations and Stephan-Maxwell equations were compared for the simulation of hydrogen production in microreactors. The reaction used for hydrogen production was methanol steam reforming. In most of the literature reviewed herein, mixture average correlations were used for the simulation of hydrogen production. However, the results indicated that mixture average correlations caused a higher relative error in temperature profile than Stephan-Maxwell equations at all the flow rates. Furthermore, considering the difference in temperature profiles confirmed the necessity of using Stephan-Maxwell equations for the simulation. It should be noted that Stephan-Maxwell equations increase the required calculations and computation time but lead to more accurate results. To develop this study, the investigation of different flow rates and geometries is proposed.

Nomenclature

C_k	: Concentration of *k* species in gas bulk
C_{ks}	: Molar concentration of *k* species in catalyst surface
C_p	: Heat capacity of gas
C_{pk}	: Heat capacity of *k* species
d_i	: Driving force mass transfer of *i* species
D_{kJ}	: Molecular diffusion coefficient of *k* species in *J*
D_{km}	: Average molecular diffusion coefficients of *k* species in bulk fluid
E	: Total energy of gas
E_{ai}	: Activation energy
F	: Volumetric flow rate (feed)
H	: Enthalpy
J_k	: Molecular flux of *k* species
K	: Thermal conductivity
K_{ck}	: Mass transfer coefficient of *k* species
K_{i0}	: Frequency factor
K_k	: Thermal conductivity of *k* species
M_k	: Mass fraction of *k* species
M_{mean}	: Average molecular mass
P	: The total pressure of the gas mixture
$''q$	: External heat flux
Q_R	: Heat of reaction
r	: Reaction rate
R	: Universal gas constant
R_k	: Surface reaction rate of *k* species
S/C	: Steam to carbon ratio
T	: Temperature
U	: Internal energy
u_{in}	: Feed rate
u_k	: Speed of *k* species
V	: Special volume of gas
X_J	: Mole fraction of *J* species

References

Bader, G. and Deuflhard, P. A., Semi-implicit Mid-point Rule for Stiff Systems of Ordinary Differential Equations, Number Math, Vol. 41, p. 373-398, 1983.

Binlin, D. and Yongchen, S., A CFD Approach on Simulation of Hydrogen Production from Steam Reforming of Glycerol in a Fluidized Bed Reactor, International Journal of Hydrogen Energy, Vol. 35, p. 10271-10284, 2010.

Ding, O. L. and Chan, S. H., Auto Thermal Reforming of Methane Gas Modelling and Experimental

Validation, International Journal of Hydrogen Energy, Vol. 33, p. 633-43, 2008.

Fang, X. C. and Hu, Y. K., Development of Hydrogenation Technology, Petrochemical Technology, Vol. 14, p. 13-8, 2006.

Fazeli, A. and Behnam., Hydrogen Production in a Zigzag and Straight Catalytic Wall Coated Micro Channel Reactor by CFD Modelling, International Journal of Hydrogen Energy, Vol. 35, p. 9496-9503, 2010.

Fukahori, S., Koga, H., Kitaoka, T., Nakamura, M., and Wariishi, H., Steam Reforming Behaviour of Methanol Using Paper-structured Catalysts: Experimental and Computational Fluid Dynamic Analysis, International Journal of Hydrogen Energy, Vol. 33, p. 1661-1670, 2008.

Gallucci, F. and Basile. A., PdeAg Membrane Reactor for Steam Reforming Reactions: a Comparison between Different Fuels, International Journal of Hydrogen Energy, Vol. 33, p. 1671-87, 2008.

Irani, M., Alizadehdakhel, A., Nakhaei Pour, A., Hoseini, N., and Adinehnia, M., CFD Modelling of Hydrogen Production Using Steam Reforming of Methane in Monolith Reactors: Surface or Volume-base Reaction Model?, International Journal of Hydrogen Energy, Vol. 36, p. 15602-15610, 2011.

Kawamura, Y., Ogura, N., Yamamoto, T., and Igarashi, A., Aminiaturized Methanol Reformer with Si Based Micro Reactor for a Small PEMFC, Chemical Engineering Science, Vol. 61, p.1092–1101, 2005.

Kim, T. and Kwon, S., Design Fabrication and Testing of a Catalytic Microreactor for Hydrogen Production, Journal of Micromechanics and Microengineering, Vol. 16, p. 1760-1768, 2006.

Liao, C. and Erickson, P. A., Characteristic Time as a Descriptive Parameter in Steam Reformation Hydrogen Production Processes, International Journal of Hydrogen Energy, Vol. 33, p. 1652-60, 2008.

Mizsey, P., Newson, E., Truong, T. B., and Hottinger, P., The Kinetics of Methanol Decomposition: a Part of Autothermal Partial Oxidation to Produce Hydrogen for Fuel Cells, Applied Catalysis A: General, Vol. 213, p. 233-237, 2010.

Pattekar, A. V. and Kothare, M. V., A Micro-reactor for In Situ Hydrogen Production by Catalytic Methanol Reforming, International Conference on Microreaction Technology, p. 27-30, 2001.

Sharma, P. O., Abraham, M. A., and Chattopadhyay, S., Development of a Novel Metal Monolith Catalyst for Natural Gas Steam Reforming, Industrial & Engineering Chemistry Research, Vol. 46, p. 9053-9060, 2007.

Suh, J. S., Lee, M., Greif, R., and Grigoropoulos, C., Transport Phenomena in a Steam-methanol Reforming Micro Reactor with Internal Heating, International Journal Hydrogen Energy, Vol. 34, p. 314-322, 2009.

Terazaki, T., Masatos, V., Keishi, T., Osamu, T., and Tadao, Y., Development of Multi-layered Microreactor with Methanol Reformer for Small PEMFC, Journal of Power Sources, Vol. 145, p. 691-696, 2005.

Vagia, E. C. and Lemonidou, A. A., Thermodynamic Analysis of Hydrogen Production via Autothermal Steam Reforming of Selected Components of Aqueous Bio-oil Fraction, International Journal of Hydrogen Energy, Vol. 33, p. 2489-500, 2008.

Xuli, Z., Shi, D., Yinhong, C., Yong, J., and Yi, C., CFD Simulation with Detailed Chemistry of Steam Reforming of Methane for Hydrogen Production in an Integrated Micro-reactor, International Journal of Hydrogen Energy, Vol. 35, p. 5383-5392, 2010.